TWMS J. App. and Eng. Math. V.11, Special Issue, 2021, pp. 248-257

NEURAL NETWORK MODELING OF CONVECTION HEAT TRANSFER COEFFICIENT FOR THE CASSON NANOfluID

M. SHANMUGAPRIYA[1] AND P. SANGEETHA[2], §

Abstract. This paper presents applications of Artificial Neural Network (ANN) to develop a mathematical model of magnetohydrodynamic (MHD) flow and heat transfer in a Casson nanofluid. The model equations are solved numerically by Runge-Kutta Fehlberg method with shooting technique. In the developing ANN model, the performance of the various configuration were compared with various types of errors such as Mean Square Error (MSE), Mean Absolute Error (MAE) and Sum Square Error (SSE). The best ANN configuration incorporated two hidden layers with twenty five neurons in each hidden layer was able to construct convective heat transfer coefficients with MSE, MAE and SSE of 0.006346, 0.009813 and 1.015423%, respectively, and had R^2 of 0.741516. A good co-relation has been obtained between the predicted results and the numerical values.

Keywords: Artificial neural network (ANN), convective heat transfer coefficient, magnetohydrodynamic, Casson nanofluid
AMS Subject Classification: 68T05, 80A20, 76W05

1. Introduction

Researchers have developed a new class of fluid called Nanofluid, which is the dispersion of nano-sized particles in a base fluid. Nanofluids have been prepared by using many types of materials such as metal, non-metal, metal oxide, carbide, carbon nanotube (CNT) and hybrid. Nanofluids are proved to exhibit higher thermal performance compare to the ordinary heat transfer fluids such as water, oil and ethylene glycol etc. (Choi [1] and Eastman et al. [2]). Heat transfer fluids play a major role in industrial heat exchangers and automobile cooling system. In the extreme cold condition, a huge amount of energy is expended for heating industrial systems. The present of EG mixed with water in different proportions as a heat transfer fluid to freeze at normal temperature of liquid water because the freezing point for EG is-13°C. The boiling point of the EG is 198°C, which is much higher than the water. Therefore, for high temperature applications in industrial heat exchangers, mixtures of EG and water are used to raise the aqueous boiling points. With addition of nanoparticles with high thermal conductivity of the solution of EG, the thermal conductivity of the fluid is enhanced. (Beck et al. [3])

[1] Department of Mathematics, SSN College of Engineering, Chennai, India.
e-mail: mnshanpriya@yahoo.com/shanmugapriyam@ssn.edu.in
ORCID: https://orcid.org/0000-0002-2405-7402.
[2] Department of Civil Engineering, SSN College of Engineering, Chennai.
e-mail: sangeethap@ssn.edu.in; ORCID: https://orcid.org/0000-0002-7630-011X.
§ Manuscript received: October 19, 2019; accepted: April 2, 2020.

Beck et al [4] investigated that the Nanofluid consisting of metal oxide such as Aluminum oxide (Al_2O_3), Copper oxide (CuO) and Silicon oxide (SiO_2) in water, ethylene glycol and ethylene glycol+water mixtures have high thermal conductivity. Maiga et al. [5] have undertaken numerical investigations of convective heat transfer of the forced convective flows with the properties of (Al_2O_3) nanofluids using water and ethylene glycol as a base fluid, and it was found that Al_2O_3/EG has better heat transfer enhancement than Al_2O_3/water. Research undertaken by [6]-[9] has analyzed the viscosity and thermal conductivity of ethylene glycol base nanofluids. They observed that dispersing various types of metal oxide such as Copper oxide (CuO), Aluminum oxide (Al_2O_3) and Titanium oxide (TiO_2) lead to an anomalously increased thermal physical property of ethylene glycol-based nanofluids. The focus of our study is to make observations about the boundary layer flow and heat transfer in the Casson nanofluid taking into account the effect of MHD with thermal radiation and heat generation over an unsteady stretching sheet.

2. Mathematical formulations

Consider the transient two-dimensional laminar MHD flow and heat transfer of an incompressible Casson nanofluid past a stretching sheet with stretching velocity $u_w(x,t) = \frac{ax}{1-\lambda t}$ where $a(>0)$ being the stretching constant and the free stream velocity $u_e(x,t) = \frac{bx}{1-\lambda t}$ where $b(>0)$ being the strength of the stagnation point. The stream function ψ can be defined as $u = \frac{\partial \psi}{\partial y}$ and $v = -\frac{\partial \psi}{\partial x}$. Similarly, the temperature at the surface and free stream are denoted as $T_w(x,t) = T_\infty + \frac{ax^2}{(1-\lambda t)^2}$ and T_∞ respectively. The uniform magnetic field B_0 is applied to the flow direction. The rheological equation of state for an isotropic and incompressible flow of Casson fluid is as can be written as (Bhattacharyya [10])

$$\tau_{ij}(x) = \begin{cases} 2\left(\mu_B + \frac{p_y}{\sqrt{2\pi}}\right) e_{ij} & \text{if } \pi > \pi_c \\ 2\left(\mu_B + \frac{p_y}{\sqrt{2\pi_c}}\right) e_{ij} & \text{if } \pi < \pi_c \end{cases} \tag{1}$$

The basic governing equation of continuity, boundary layer flow and heat transfer for such type of flow are as follows:

$$\frac{\partial^2 \psi}{\partial y \partial x} - \frac{\partial^2 \psi}{\partial x \partial y} = 0 \tag{2}$$

$$\left(\frac{\partial^2 \psi}{\partial t \partial y} + \frac{\partial \psi}{\partial y}\frac{\partial^2 \psi}{\partial x \partial y} - \frac{\partial \psi}{\partial x}\frac{\partial^2 \psi}{\partial y^2}\right) = u_e \frac{\partial u_e}{\partial x} + \nu_{nf}\left(1 + \frac{1}{\beta}\right)\frac{\partial^3 \psi}{\partial y^3} - \frac{\sigma B_0^2}{\rho_{nf}}\left(\frac{\partial \psi}{\partial y} - u_e\right) \tag{3}$$

$$\left(\frac{\partial^2 \psi}{\partial t \partial y} + \frac{\partial \psi}{\partial y}\frac{\partial T}{\partial x} - \frac{\partial \psi}{\partial x}\frac{\partial T}{\partial y}\right) = \frac{k_{nf}}{(\rho c_p)_{nf}}\frac{\partial^2 T}{\partial y^2} + \frac{\nu_{nf}}{(c_p)_{nf}}\left(1 + \frac{1}{\beta}\right)\left(\frac{\partial^2 \psi}{\partial y^2}\right)^2 - \frac{1}{(\rho c_p)_{nf}}\frac{\partial q_r}{\partial y} + \frac{Q_0}{(\rho c_p)_{nf}}(T - T_\infty) \tag{4}$$

The dimensional boundary conditions are:

$$\begin{aligned} &\frac{\partial \psi}{\partial y} = u_w(x,t),\ \frac{\partial \psi}{\partial x} = 0,\ T = T_w(x,t) \text{ at } y = 0 \\ &\frac{\partial \psi}{\partial y} \to u_e(x,t),\ T \to T_\infty \text{ as } y \to \infty \end{aligned} \tag{5}$$

The relation between the physical quantities of Casson nanofluid, Ethylene Glycol, Aluminum oxide and Copper oxide are written as follows:

TABLE 1. Thermophysical properties of base fluid and nanoparticles

	$\rho(kg/m^3)$	$c_p(J/kgK)$	$k(W/mK)$
Ethylene Glycol	1114	2415	0.252
Aluminum oxide (Al_2O_3)	3970	765	40
Copper oxide (CuO)	6510	540	18

$$\mu_{nf} = \frac{\mu_f}{(1-\phi)^{2.5}},\ (\rho c_p)_{nf} = (1-\phi)(\rho c_p)_f + \phi(\rho c_p)_s,\ \frac{k_{nf}}{k_f} = \frac{(k_s+2k_f)-2\phi(k_f-k_s)}{(k_s+2k_f)+2\phi(k_f-k_s)} \quad (6)$$

Here ρ_{nf}, μ_{nf}, k_{nf}, $(\rho c_p)_{nf}$ are the density, dynamic viscosity, thermal conductivity, heat capacitance of the nanofluid, k_f and k_s are the thermal conductivity of fluid and solid fraction.

The following similarity transformations are invoked:

$$\psi = \sqrt{\frac{a\nu_f}{(1-\lambda t)}} x f(\eta),\ \eta = \sqrt{\frac{a}{\nu_f(1-\lambda t)}} y,\ T = \frac{ax^2}{(1-\lambda t)^2}\theta(\eta) + T_\infty \quad (7)$$

where $f(\eta)$ and $\theta(\eta)$ are non-dimensional velocity and temperature respectively. Using these variables in Eqs.(3) and (4), we get the following nonlinear ordinary differential equations:

$$\left(1+\frac{1}{\beta}\right) f''' + (1-\phi)^{2.5}\left\{\left[(1-\phi)+\phi\left(\frac{\rho_s}{\rho_f}\right)\right]\left[ff''-(f')^2 - A(f'+\frac{\eta}{2}f'') + C^2\right]\right. \quad (8)$$
$$\left. + M(C-f')\right\} = 0$$
$$\left[\frac{k_{nf}}{k_f} + N_R\right]\theta'' - \left[(1-\phi)+\frac{(\rho c_p)_s}{(\rho c_p)_f}\phi\right] Pr\left[A\left(2\theta+\frac{\eta}{2}\theta'\right) + 2f'\theta - f\theta'\right] \quad (9)$$
$$+\frac{PrEc}{(1-\phi)^{2.5}}\left(1+\frac{1}{\beta}\right)(f'')^2 + PrHe\theta = 0$$

with boundary conditions:

$$\begin{aligned} &f(0)=0,\ f'(0)=1,\ \theta(0)=1 \text{ at } y=0 \\ &f'(\infty)=C,\ \theta(\infty)=0 \text{ as } y\to\infty \end{aligned} \quad (10)$$

where ϕ volume fraction of nanoparticles in the nanofluid, $A = \frac{\lambda}{a}$ is the unsteadiness parameter, $C = \frac{b}{a}$ is the stretching parameter, $M = \frac{\sigma B_0^2(1-\lambda t)}{\rho_{nf} a}$ is the magnetic parameter, $N_R = \frac{16\sigma^* T_\infty^3}{3k^* k_f}$ is the radiation parameter, $Pr = \frac{\nu_f}{\alpha_f}$ is the Prandtl number, $Ec = \frac{a}{(c_p)_f}$ is the Eckert number, $He = \frac{Q_0}{(\rho c_p)_f}\left(\frac{1-\lambda t}{a}\right)$ is the heat generation parameter, σ is the electrical conductivity of fluid, ν_f and α_f are the kinematic viscosity and thermal diffusivity of fluid and Q_0 is the heat generation constant.

3. Methodology

3.1. **Numerical approach.** The system of coupled nonlinear ordinary differential equations and their corresponding boundary conditions (8)-(10) is solved numerically by Runge-Kutta Fehlberg method with shooting technique. In order to check the accuracy and validation of our MATLAB code, the values of friction factor are compared with the previous published work and are found to be good agreement (Table 2).

Table 2. Comparison of the presently computed values of $f''(0)$ with those of existing literature for different values of C when $\beta \to \infty$.

C	Present	Oyelakin et al. [11]	Mustafa et al. [12]	Ishak et al. [13]
0.01	-0.9981	-0.9978	-0.9980	-0.9980
0.10	-0.9694	-0.9694	-0.9694	-0.9694
0.20	-0.9181	-0.9181	-0.9181	-0.9181
0.50	-0.6673	-0.6673	-0.6674	-0.6673
2.00	2.0175	2.0175	2.0176	2.0175
3.00	4.7293	4.7293	4.7296	4.7294

3.2. **Artificial Neural Network (ANN) approach.** ANN architecture consists of five major elements such as inputs, weights, sum function, activation function and outputs. The input layer gets information from outside environment and passes it on to the hidden layer where the information is processed by summing up together with bias term as given in Eq. (11)

$$y = f\left(\sum_{i=0}^{n} x_i w_i - b\right) \tag{11}$$

where f is the activation function, x_i and w_i are the i^{th} input neuron and the corresponding weight, n is the number of neurons, b is the bias term and y is the output. The most common activation function is the sigmoid function, and is expressed as in Eq. (12)

$$f(t) = \frac{1}{1+e^{-\alpha t}} \text{ where } t = \left(\sum_{i=0}^{n} x_i w_i - b\right) \tag{12}$$

where α is a constant to manage the gradient of the semi-linear region. The network forward the input signals to the next layers until desired outputs are achieved. The calculated outputs are compared with the actual values, if the errors are more than the calculated numerical values than these weights are readjusted until the errors are minimized.

3.2.1. **Construction of ANN model.** In this work, an ANN model is developed through numerical study of various physical parameters to predict the skin friction and Nusselt number coefficients. Nine different parameters were considered as input, and they are $A, \phi, \beta, C, M, N_R, Pr, Ec$ and He, the skin friction and the Nusselt numbers of the MHD Flow of Ethylene Glycol-Based Casson Type Nanofluid over an Unsteady Stretching Sheet were the target output. Levenberg - Marquardt training algorithm was used in the present

study. The range of input and output variables considered are given in Table 3. The architecture of the proposed ANN model is shown in Figure 1.

TABLE 3. ANN's input and output attributes

SI.No	Input and output attributes	Range	Remarks
1	Unsteadiness parameter (A)	0.7-1.7	Input
2	Volume fraction parameter (ϕ)	0.01-0.2	
3	Non-Newtonian Casson parameter (β)	0.1-1.5	
4	Stretching parameter (C)	0.1	
5	Magnetic parameter (M)	0.1-2.5	
6	Radiation parameter (N_R)	1.0-5.0	
7	Prandtl number (Pr)	0.1-1.0	
8	Eckert number (Ec)	0.1-0.5	
9	Heat generation parameter (He)	0.1-0.5	
10	Skin friction (Al_2O_3)		Output
11	Nusselt number (Al_2O_3)		
12	Skin friction (CuO)		
13	Nusselt number (CuO)		

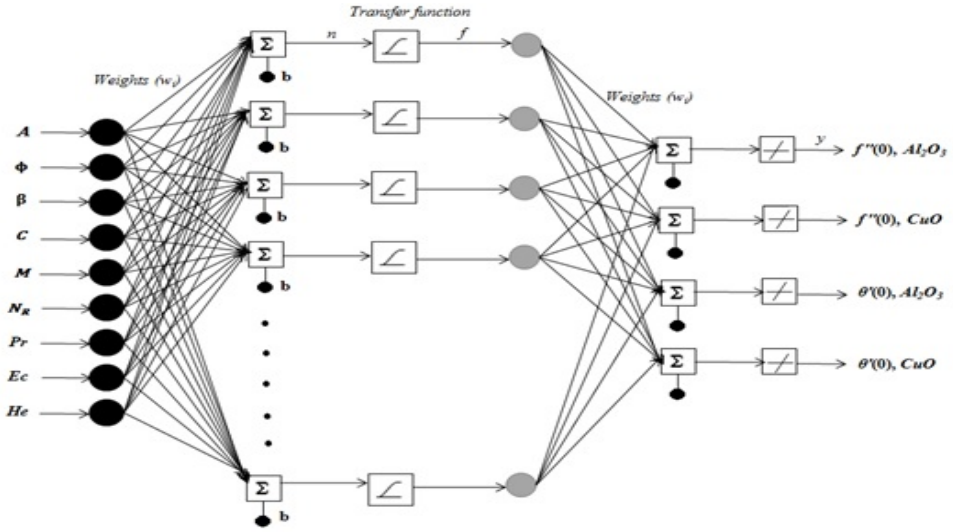

FIGURE 1. A simplified outline of the suggested ANN model

The ANN configuration was trained using the input data in order to accomplish reliable prediction of the targeted output. Normally, the data would be divided in to three subsets: 70% for training, 15% for testing and 15% for validating. The performance of the various ANN configuration were compared with various types of errors such as Mean Square Error (MSE), Mean Absolute Error (MAE) and Sum Square Error (SSE) given by Eqs. (13) - (15). The coefficient of determination R^2, of the linear regression line between the predicted values from the ANN model and the desired output was also used as a measure of performance.

$$MSE = \sqrt{(M_{cal} - M_{pred})}/M_{cal} \quad (13)$$

$$MAE = \sum (M_{cal} - M_{pred}) \quad (14)$$

$$SSE = \sqrt{\sum (M_{cal} - M_{pred})^2}/N - 1 \quad (15)$$

where M_{cal}=calculated output by numerical method, M_{pred}=predicted value by ANN model and N=number of data point.

TABLE 4. Error parameter in the prediction of skin friction and Nusselt number coefficients

No. of neurons in each hidden layer	MSE(%)	MAE(%)	SSE(%)	R^2
1	0.013175	0.061289	2.107993	5.833268
5	0.007196	0.034333	1.151396	0.706903
10	0.006638	0.017831	1.062145	0.729622
15	0.008106	0.037508	1.297000	0.669838
20	0.011216	0.052882	1.794607	0.543168
23	0.006346	0.009813	1.015423	0.741516*
25	0.036458	0.124575	1.833268	-0.48491

The ANN model with one hidden layer and different neuron in each layer predicted skin friction and Nusselt number coefficients with MSE, MAE, SSE and R^2, as shown in Table 4. From this table, the best ANN configuration included one hidden layer with twenty-three neurons in each layer. The MSE, MAE and SSE for this optimal configuration with different neural networks were 0.006346, 0.009813 and 1.015423%, respectively, and had R^2 of 0.741516.

4. Discussion of results

TABLE 5. Numerical and predicted skin friction

ϕ	A	C	M	β	N_R	Pr	Ec	He	NM		ANN	
									Al_2O_3	CuO	Al_2O_3	CuO
0.01	1.2	0.1	0.5	0.5	1	0.72	0.1	0.1	-0.8703	-0.8783	-0.8697	-0.8784
0.05									-0.8600	-0.8958	-0.8599	-0.8959
0.1									-0.8413	-0.9042	-0.8411	-0.9043
0.15									-0.8166	-0.8998	-0.8169	-0.8996
0.2									-0.7868	-0.8846	-0.7871	-0.8847
0.05	1								-0.8294	-0.8635	-0.8288	-0.8630
	1.2	0.1	0.5						-0.8600	-0.8958	-0.8599	-0.8959
				0.3					-0.7153	-0.7451	-0.7146	-0.7453
				0.5	3				-0.8600	-0.8958	-0.8596	-0.8958
					1	1			-0.8600	-0.8958	-0.8202	-0.8705
						0.72	0.5		-0.8600	-0.8958	-0.8599	-0.8957
							0.1	0.3	-0.8600	-0.8958	-0.8623	-0.9010

In this study the governing equations were solved using Runge-Kutta Fehlberg method with shooting technique. Extensive numerical simulations have been performed to obtain the velocity and temperature profiles as well as skin friction and Nusselt number for

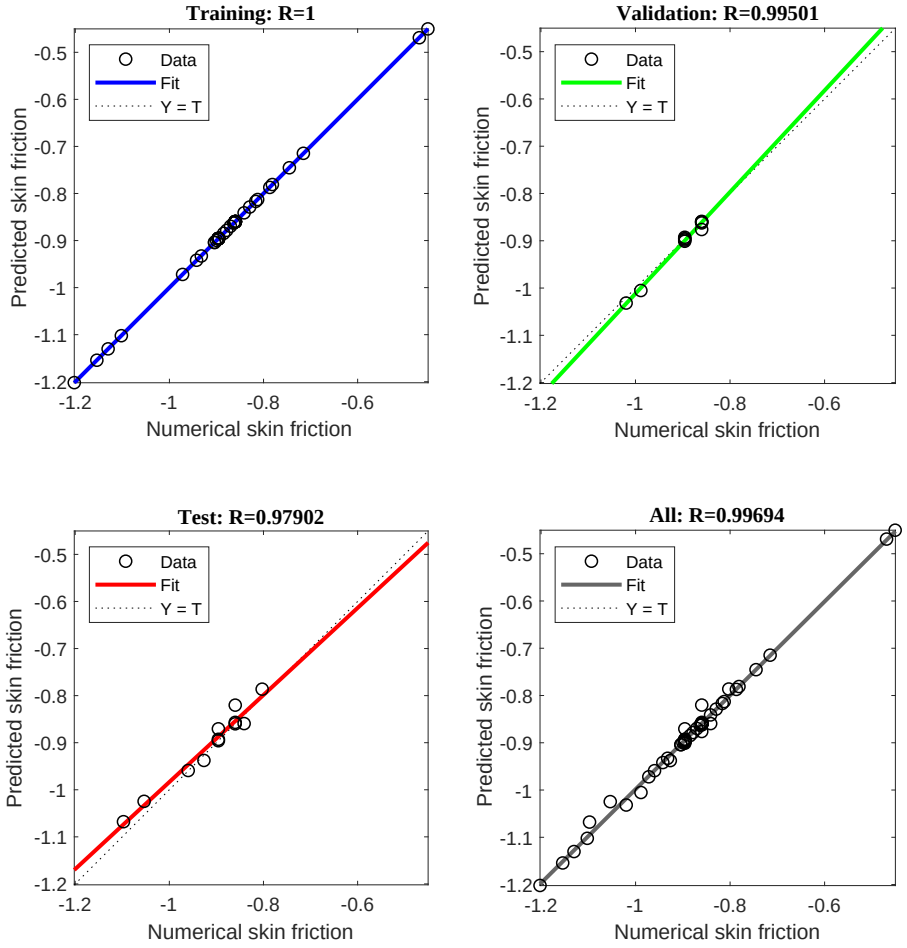

FIGURE 2. Optimum ANN predicted values verses numerical values of skin friction coefficient

various physical parameters. The total 80 numerical results were used to train, validate and test the ANN model for the friction coefficient. Table 5 and 6 show the comparison sample of friction factor and Nusselt number of Aluminum oxide (Al_2O_3)/Ethylene Glycol (EG) and Copper oxide (CuO)/Ethylene Glycol (EG) nanofluids that calculated by ANN model and numerical method. It is observed that the enhancement of skin friction and Nusselt number coefficient appears clearly more pronounced for CuO/EG nanofluids than for $Al_2O_3/(EG)$ nanofluids. Also the nanofluid volume fraction parameter (ϕ) increases, skin friction and Nusselt number coefficient increases.

The 48 data set were used for the training set, 12 data sets were used for validation and the rest of the data were used for testing the results of the ANN model. The performances of skin friction and Nusselt number for training, validation and test sets of the proposed ANN model is shown in Figs. 2, 3 respectively. It is observed that there are good agreement between ANN model and numerical analysis for both friction factor and Nusselt number data with R square value 92%.

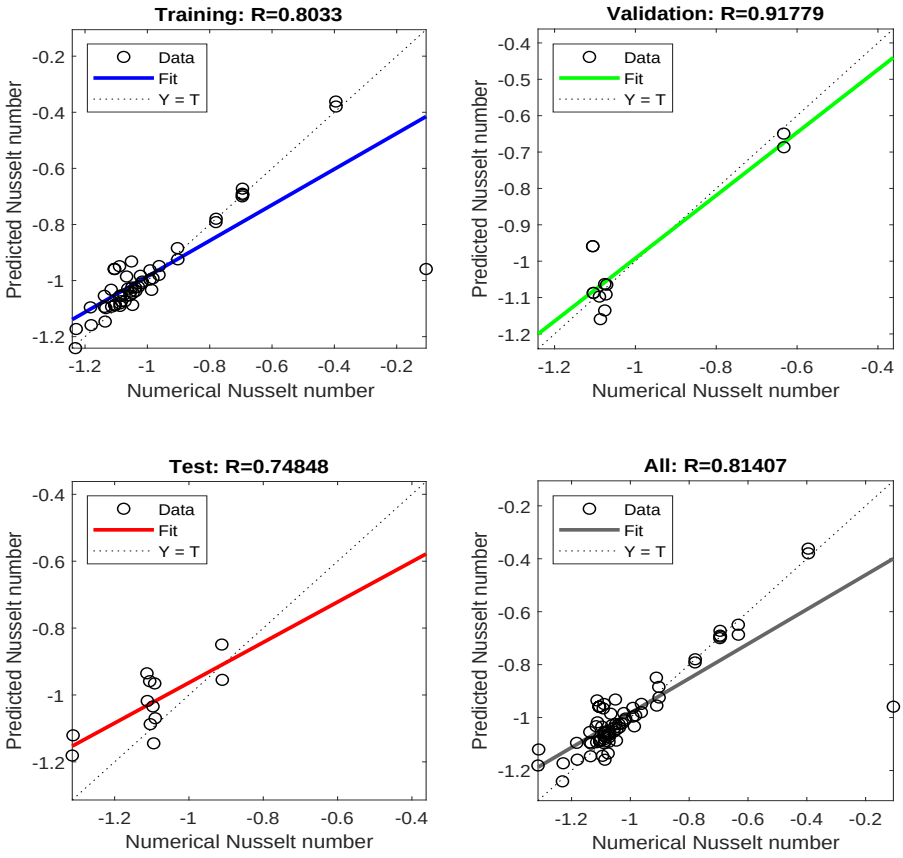

FIGURE 3. Optimum ANN predicted values verses numerical values of Nusselt number coefficient

TABLE 6. Numerical and predicted Nusselt number

ϕ	A	C	M	β	N_R	Pr	Ec	He	NM		ANN	
									Al_2O_3	CuO	Al_2O_3	CuO
0.01	1.2	0.1	0.5	0.5	1	0.72	0.1	0.1	-1.1374	-1.1377	-1.0938	-1.0544
0.05									-1.1039	-1.1056	-1.0873	-0.9588
0.1									-1.0628	-1.0667	-1.0289	-0.9855
0.15									-1.0223	-1.0288	-0.9829	-1.0225
0.2									-0.9824	-0.9916	-0.9918	-0.9964
0.05	1								-1.0497	-1.0510	-1.0248	-0.9319
	1.2	0.1	0.5						-1.1039	-1.1056	-1.0873	-0.9588
				0.3					-1.1144	-1.1162	-1.0931	-1.0327
				0.5	3				-0.7795	-0.7802	-0.7797	-0.7917
					1	1			-1.3119	-1.3140	-1.1206	-1.1811
						0.72	0.5		-0.9913	-0.9865	-0.9633	-1.0332
							0.1	0.3	-1.0712	-1.0729	-1.0646	-1.0914

5. CONCLUSIONS

The convective heat transfer characteristic of Aluminum oxide (Al_2O_3)/Ethylene Glycol (EG) and Copper oxide (CuO)/Ethylene Glycol (EG) nanofluids have been investigated.

The velocity and temperature profiles as well as friction factor and heat transfer coefficient were measured. The following conclusions are drawn from this study (i) the velocity and temperature profiles increases with the increasing values of the volume fraction of nanoparticles in the nanofluid (ii) increasing the unsteadiness parameter reduces the velocity and temperature profiles. (iii) Casson parameter and magnetic field parameter have similar impact on velocity profile but they do have opposite effects on temperature profile (iv) radiation and heat generation parameter have improves the effect of dimensionless temperature (v) results have clearly revealed that heat transfer argumentation of Ethylene Glycol as a base fluid appears to be more pronounced than water. Also the increment of heat transfer coefficient is higher in CuO/EG nanofluids compared to Al_2O_3/EG nanofluids.

Acknowledgement. The authors would like to thank the Management and Principal, SSN College of Engineering, Chennai, India.

References

[1] Choi, U. S. (1995), Enchancing thermal conductivity of fluids with nanoparticles. in:D.A.Siginer, H.P.Wang (Eds.), Developments and Applications of Non-Newtonian Flows, American Society of Mechanical Engineers (ASME), New York, Vol. FED-Vol.231/MD-Vol.66, 99-105.

[2] Eastman, J. A., Choi, S. U. S., Li, S., Thompson, L. J., & Lee, S. (1997), Enhanced thermal conductivity through the development of nanofluids. Proc. Symposium Nanophase and Nano composite Materials II, 457, 3-11.

[3] Beck, M. P., Sun, T., & Teja, A. S. (2007), The thermal conductivity of alumina nanoparticles disperses in ethylene glycol. Fluid Phase Equilib., 260, (2), 275-278.

[4] Beck, M. P., Yuan, Y., Warrier, P., Amyn, S., & Teja, A.S. (2010), The thermal conductivity of alumina nanofluids in water, ethylene glycol and water ethylene glycol mixtures. J. Nanopart. Res., 12, 1469-1477.

[5] Maiga, S., EI, B., Palm, S. J., Nguyen, C. T., Roy, G., & Galanis, N. (2005), Heat transfer enhancement by using nanofluids in forced convection flows. Int. J. Heat Mass Transfer, 26, (4), 530-546.

[6] Kwak, K., & Chongyoup, K. (2005), Viscosity and thermal conductivity of copper oxide nanofluid dispersed in ethylene glycol. Korea-Aust. Rheol. J., 17, (2), 35-40.

[7] Pastoriza-Gallego, M., Lugo, L., Legido, J., & Piñeiro, M. (2011), Thermal conductivity and viscosity measurements of ethylene glycol-based Al2O3 nanofluids. Nanoscale Res. Lett., 6, (221), 1-11.

[8] Chen, H., Ding, Y., Lapkin, A., & Fan, X. (2009), Rheological behaviour of ethylene glycol-titanate nanotube nanofluids. J. Nanopart. Res., 11, (6), 1513-1520.

[9] Reddy, M., Chandra, S., Rao, V., Reddy, B., Chandra, M., Sarada, S. N., & Ramesh, L. (2012), Thermal conductivity measurements of ethylene glycol water based TiO2 nanofluids. Nanosci. Nanotechnol. Lett. 4, (1), 105-109.

[10] Bhattacharyya , K. (2013), MHD stagnation-point flow of Casson fluid and heat transfer over a stretching sheet with thermal radiation. J. Therm., 2013.

[11] Oyelakin, I. S., Mondal, S., & Sibanda, P., (2016), Unsteady Casson nanofluid flow over a stretching sheet with thermal radiation, convective and slip boundary conditions. Alexandria Engineering Journal, 55, 1025-1035.

[12] Mustafa, M., Hayat, T., Pop, I., & Hendi, A. (2011), Stagnation-point flow and heat transfer of a Casson fluid towards a stretching sheet. Z. Naturforsch., 67a, 70-76.

[13] Ishak, A., Nazar, R., Arifin, N. M., & Pop I. (2007), Mixed convection of the stagnation-point flow towards a stretching vertical permeable sheet. Malay. J. Math. Sci., 1, 217-226.

Dr. M. Shanmugapriya is an assistant professor in the Department of Mathematics. She received her doctoral degree from Anna University specializing in Fluid Mechanics, master's degree from Madurai Kamaraj University and bachelor's degree from Gandhigram Deemed University. Her research interests include Computational Fluid Mechanics, Heat and Mass Transfer, MHD flow, Newtonian and non-Newtonian flow and Artificial intelligence. She is carrying out a 3-year project titled "Prediction of Mechanical Properties of Nano-Concrete Using Artificial Neutral Networks and Fuzzy Logic" with a budget of 5.5 lakh funded by SSN Trust.

Dr. P. Sangeetha is an associate professor in the Department of Civil Engineering. She completed her B.E (Civil), MS (Research), and Ph.D from college of Engineering, Guindy, Anna University. Her area of interest includes composite space truss, steel concrete composite, cold formed steel sections and finite element analysis.